

Long Baseline Neutrino Experiments and the LOW solution – What is Left to Do and How Well Can It Be Done

Gabriela Barenboim and André de Gouvêa
Theoretical Physics Division, Fermilab, P.O. Box 500, Batavia, IL, 60510-0500, USA

The neutrino community is convinced that if the LMA solution is indeed correct, the prospects for next-generation, long-baseline neutrino experiments are very exciting. In this work we will argue that the prospects are not less exciting if the answer to the solar neutrino puzzle lies in the LOW region. For this purpose we explore the oscillation probabilities which are accessible to experiments which employ conventional neutrino beams. We consider the electron (anti)neutrino appearance channel, which provides information regarding not only the small U_{e3} -element of the leptonic mixing matrix but also the neutrino mass hierarchy, and also include information, which should come from the muon (anti)neutrino disappearance channel, regarding the magnitude of the atmospheric mass-squared difference (Δm_{13}^2) and mixing angle (θ_{23}). We comment on the presence of ambiguities and the experiments needed to solve them.

1. INTRODUCTION

There is unambiguous evidence of new physics in the leptonic sector of the standard model. Furthermore, all experimental neutrino data [1, 2, 3, 4, 5] are consistent with the hypothesis that neutrinos have mass and mix. This being the case, the goal of this and the next generation of neutrino experiments is to determine the neutrino masses and the leptonic mixing matrix to the best of their capabilities.

One of the issues which is to be resolved by the present generation of neutrino experiments involves the determination of the so-called solar parameters, Δm_{12}^2 and $\tan^2 \theta_{12}$. The current data strongly require $\tan^2 \theta_{12}$ to be of order unity, while $10^{-4} \text{ eV}^2 \lesssim \Delta m_{12}^2 \lesssim 10^{-5} \text{ eV}^2$ (the large mixing angle solution (LMA)) or $\Delta m_{12}^2 \ll 10^{-6} \text{ eV}^2$ [2, 6, 7]. The latter will be referred to in this paper as the LOW solution.* While global analyses indicate that the LMA solution is significantly preferred, it is fair to say that the LOW solution still remains a realistic possibility [8].

In any case, the KamLAND reactor neutrino experiment [9] will, in the near future, definitively establish whether the LMA solution is driving solar neutrino oscillations. If KamLAND observes an oscillation signal, it will not only exclusively select the LMA solution but also “pin-point” the value of solar parameters [10, 11]. If KamLAND does not observe an oscillation signal, the LMA solution will be unambiguously (modulo CPT violation [12]) ruled out [11], and we will have to wait for the Borexino solar neutrino experiment [13], which is scheduled to start data-taking in 2003, in order to definitively piece the solar neutrino puzzle [14].

If the LMA solution is indeed correct, the prospects for next-generation, long-baseline neutrino experiments are very exciting. Not only can these experiments probe the remaining mixing angle of the leptonic mixing matrix, but there remains the possibility of also observing CP-violating effects. This scenario has been thoroughly studied, for different long-baseline experiments (superbeams, neutrino factories, etc), in the literature [15, 16, 17].

In this work we will explore the physics capabilities of future long-baseline oscillation experiments if the LMA solution is not correct. We will argue that a rich physics program lies ahead despite the fact that the door to leptonic CP violation will be closed (indeed, the study of any “solar effect” in terrestrial oscillation experiments becomes virtually impossible). First, we discuss the oscillation probabilities which are accessible to experiments which employ conventional neutrino beams (which are mostly composed of muon-type (anti)neutrinos). We consider both the electron (anti)neutrino appearance channel, which provides information regarding not only the small U_{e3} -element of the leptonic mixing matrix but also the neutrino mass hierarchy, and the muon (anti)neutrino disappearance channel, which provides information regarding the magnitude of the atmospheric mass-squared difference (Δm_{13}^2) and mixing angle (θ_{23}). A comparison of both expressions reveals that the information provided by the disappearance channel leads to “ambiguities” [18] in the determination of the currently unknown oscillation parameters. Far from being a nuisance, these degeneracies are an indication that more physical quantities can be measured given the correct amount of information.

Next, we simulate and analyse “data” from a finely segmented iron-scintillator detector located off-axis from the future NuMI beam at Fermilab. In measuring the oscillation parameters, we include the realistic uncertainties on all relevant parameters, and consider several scenarios in order to fully study all degeneracy issues. We find that one

* The current data allow, at the “three sigma” level, not only the LMA solution, but also the LOW, QVO, and VAC solutions, depending on the data analysis. See, [2, 6, 7] for details.

should be able to determine the neutrino mass-hierarchy by combining information from neutrino and antineutrino oscillations if $|U_{e3}|^2$ is large enough (solving one “degeneracy issue”), but not whether θ_{23} is less than or greater than $\pi/4$. We comment on how this degeneracy might be attacked. Finally, we analyse the issue of how well the atmospheric mass-squared difference should be known before choosing the location of the off-axis detector.

II. THE DISAPPEARANCE CHANNEL

We are interested in baselines around 10^3 km and order 1 GeV neutrinos energies, chosen in order to explore the first oscillation peak. We hope to show, contrary to some claims, that there is no need to go beyond the first peak in order to disentangle the oscillation features. For this class of experiments, the parameter α (see Appendix A), which measures the strength of matter effects, is given by

$$\alpha \equiv \frac{2\sqrt{2}G_F n_e E}{\Delta m_{13}^2} \simeq \frac{2.8 \cdot 10^{-4}}{\Delta m_{13}^2} \left(\frac{E}{\text{GeV}} \right), \quad (\text{II.1})$$

where n_e is the electron number density in the Earth and E is the energy of the neutrino (see Appendix A for definitions and conventions).

In the region of interest, α is relatively small ($\alpha \simeq .1 - .2$) such that, up to quartic terms in $|U_{e3}| \equiv s_{13}$, the muon neutrino survival probability can be written as (complete formulas are given in Appendix A)

$$P(\nu_\mu \rightarrow \nu_\mu) = 1 - 4s_{23}^2 c_{23}^2 c_{13}^4 \sin^2[\Delta_{13}] - s_{23}^2 \frac{4s_{13}^2}{(1-\alpha)^2} \sin^2[\Delta_{13}(1-\alpha)]. \quad (\text{II.2})$$

Note that we have also expanded $\tilde{\Delta}_{13} = \Delta_{13}[1 - \alpha](1 + O(\alpha|U_{e3}|^2))$. Matter effects, therefore, only modify the vacuum survival probability by terms which are $O(|U_{e3}|^2\alpha)$, and can safely be neglected. The vacuum expression can be written as

$$P(\nu_\mu \rightarrow \nu_\mu) = P(\bar{\nu}_\mu \rightarrow \bar{\nu}_\mu) = 1 - 4|U_{\mu 3}|^2(1 - |U_{\mu 3}|^2) \sin^2(\Delta_{13}); \quad (\text{II.3})$$

$$|U_{\mu 3}| = \sin \theta_{23} \cos \theta_{13}, \quad (\text{II.4})$$

meaning that one can measure $|\Delta m_{13}^2|$ (from the oscillation frequency) and $\sin^2 2\theta_{23}^{\text{eff}} \equiv 4|U_{\mu 3}|^2(1 - |U_{\mu 3}|^2)$ (from the magnitude of the oscillation). For $|U_{e3}| \ll 1$

$$\sin^2 2\theta_{23}^{\text{eff}} = \sin^2 2\theta_{23} \left[1 - |U_{e3}|^2 \frac{2(1 - \cos 2\theta_{23}) \cos 2\theta_{23}}{\sin^2 2\theta_{23}} + O(|U_{e3}|^4) \right]. \quad (\text{II.5})$$

In the limit of vanishing $|U_{e3}|$, $\sin^2 2\theta_{23}^{\text{eff}} = \sin^2 2\theta_{23}$, while a precise enough extraction of $\sin^2 2\theta_{23}$ from $\sin^2 2\theta_{23}^{\text{eff}}$ is sensitive to the value of $|U_{e3}|$. Indeed, the fact that $|U_{e3}|^2$ is not known induces an irreducible uncertainty on extracting $\sin^2 2\theta_{23}$ from ν_μ disappearance experiments as large as $\Delta(\sin^2 2\theta_{23}) \sim 0.02$, depending on the value of $\sin^2 2\theta_{23}$ and the uncertainty on $|U_{e3}|^2$.[†]

The information needed in order to interpret the ν_e appearance channel (as will be discussed in the next section) is $\sin^2 \theta_{23}$ (not $\sin^2 2\theta_{23}$) and (Δm_{13}^2) (not $|\Delta m_{13}^2|$). This implies that, as far as the appearance channel is concerned, the information from the disappearance channel is *four-fold degenerate*, meaning that a unique measurement of $(\sin^2 2\theta_{23}^{\text{eff}}, |\Delta m_{13}^2|)$ “splits” into

$$(\sin^2 \theta_{23}, \Delta m_{13}^2) = \left(\frac{1}{2} \left(1 \mp \sqrt{1 - \sin^2 2\theta_{23}^{\text{eff}}} \right), \pm |\Delta m_{13}^2| \right), \quad (\text{II.6})$$

where the subleading $|U_{e3}|^2$ effects have been ignored.

This parameter degeneracy is depicted in Fig. 1, where we present the one and three sigma confidence level (CL) contours in the $(\sin^2 \theta_{23} \times |U_{e3}|^2)$ and $(\sin^2 \theta_{23} \times \Delta m_{13}^2)$ -planes, assuming that one has measured $|\Delta m_{13}^2| = (3 \pm 0.1) \times 10^{-3} \text{ eV}^2$ and $\sin^2 2\theta_{23}^{\text{eff}} = 0.91 \pm 0.01$ (to be exact, the input point corresponds to $\sin^2 \theta_{23} = 0.35$ and $|U_{e3}|^2 = 0.01$, as indicated by the (blue) stars in Fig. 1). We also impose the CHOOZ bound [19] as a hard cutoff, $|U_{e3}|^2 < 0.05$,

[†] It is curious to note that for “maximal mixing” in the atmospheric sector ($\theta_{23} = \pi/4$), there are only $|U_{e3}|^4$ corrections.

and that the measurements of the effective atmospheric angle and the absolute value of the atmospheric mass-squared difference are uncorrelated. This is a simplifying assumption, which would be a good approximation if future long-baseline ν_μ disappearance experiments run at distances and energies which are around the minimum of the ν_μ survival probability. In this case, and assuming a good energy resolution and calibration, the mass-squared difference can be obtained by the position of the minimum, while the $\sin^2 2\theta_{23}^{\text{eff}}$ is obtained by the magnitude of the suppression. The capabilities of long-baseline experiments to measure the atmospheric parameters is currently under investigation [20], and clearly depend on the detector-type and the neutrino beam.

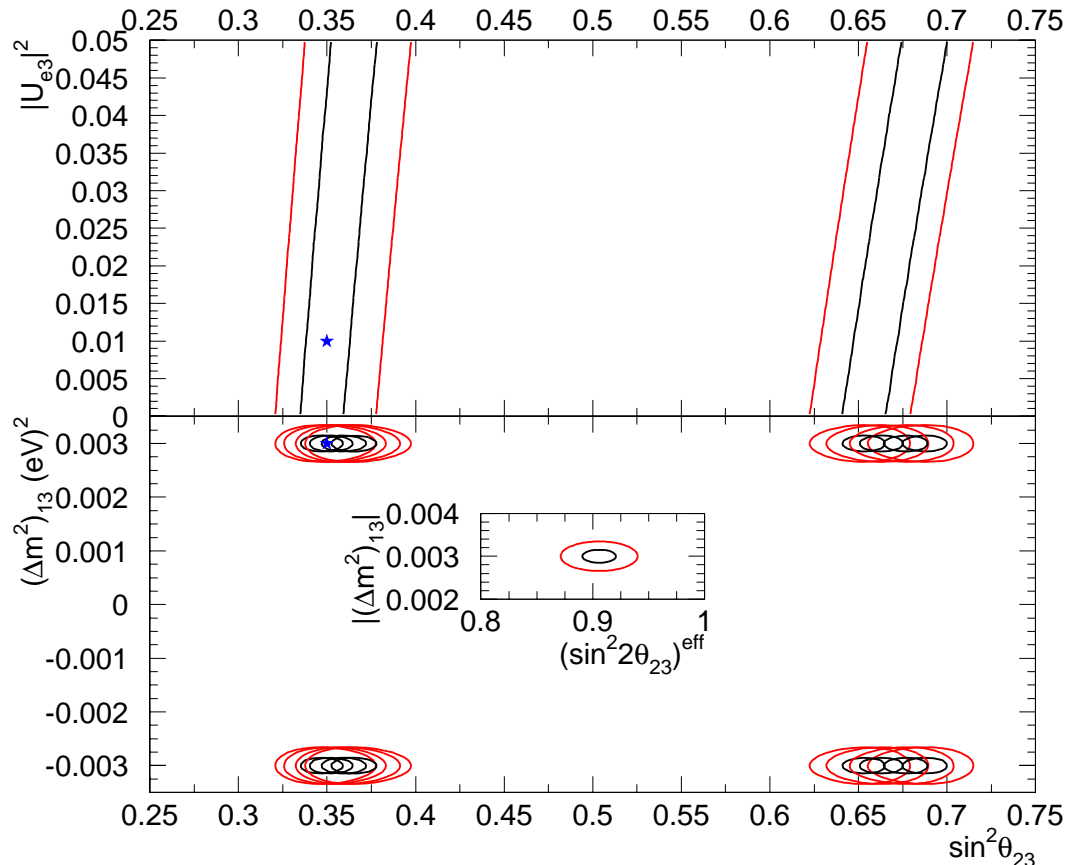


FIG. 1: One and three sigma confidence level contours in the $(\sin^2 \theta_{23} \times |U_{e3}|^2)$ and $(\sin^2 \theta_{23} \times \Delta m_{13}^2)$ -planes, obtained from the “measurement” $|\Delta m_{13}^2| = (3 \pm 0.1) \times 10^{-3} \text{ eV}^2$ and $\sin^2 2\theta_{23}^{\text{eff}} = 0.91 \pm 0.01$, depicted in the inset located in the center. See text for details.

In each plot of Fig. 1, the CLs are defined for two degrees of freedom, *i.e.*, the absent parameter in each figure has been “integrated out.” On the bottom plot, we present the confidence ellipses for different fixed values of $|U_{e3}|^2$. The appropriate one and three sigma level regions are to be interpreted as the envelope of the different inner and outer ellipses, respectively.

Several comments are in order. First, the alluded to four-fold degeneracy is clearly visible in the bottom plot of Fig. 1. Second, the fact that $|U_{e3}|^2$ is not known implies a significant increase of $\Delta(\sin^2 \theta_{23})$, as can be observed by comparing each individual ellipse in the bottom plot with the size of the envelope. The situation will improve once more information (from the appearance channel) regarding the magnitude of U_{e3} is included.

To conclude this section, we point out the simple but important fact that a Gaussian measurement of $\sin^2 2\theta_{23}^{\text{eff}}$ does *not* translate into a Gaussian measurement of $\sin^2 \theta_{23}$. This is true even when $|U_{e3}| = 0$. This can be easily understood in the following way. If the measurement of $\sin^2 2\theta$ is Gaussian, it can be transformed into a χ^2 function

$(\sin^2 2\theta - x)^2/(\sigma_x)^2$, where $x = \sin^2 2\theta^*$ is the measured value of $\sin^2 \theta$ with error $\pm\sigma_x$. This translates into

$$\chi^2(\sin^2 \theta) = \frac{((\sin^2 \theta - y_1)^2 (\sin^2 \theta - y_2)^2)}{(\sigma_x/4)^2}, \quad (\text{II.7})$$

where $y_{1,2}$ are the solutions to $y(1-y) - x/4 = 0$. If $y_{1,2}$ are separated enough (in units of σ_x) the χ^2 splits into the sum of two parabola, with error $\sigma_y = \sigma_x/|4(y_1 - y_2)|$ (of course, $|y_1 - y_2| = |\cos 2\theta^*|$). This will not be the case of maximal mixing ($y_1 = y_2 = 0.5$), where the χ^2 function will be a quartic monomial which cannot be approximated by a parabola. This implies that a measurement of $\sin^2 2\theta = 1$ with an uncertainty of 0.01 will imply $\sin^2 \theta = 0.5 \pm 0.05$, but the ± 0.05 one sigma uncertainty is very non-Gaussian, meaning that, for example, the three sigma error bar is not ± 0.15 (as a matter of fact, the three sigma error bar is significantly smaller than ± 0.15).

III. THE APPEARANCE CHANNEL

The electron neutrino appearance probability is given by (again, for small α)

$$P(\nu_\mu \rightarrow \nu_e) = s_{23}^2 \frac{4s_{13}^2}{(1-\alpha)^2} \sin^2 [\Delta_{13}(1-\alpha)], \quad (\text{III.8})$$

while the approximate expression for antineutrinos is given by Eq. (III.8) if one exchanges $\alpha \rightarrow -\alpha$. (For exact expressions see Appendix A). Note that Eq. (III.8) can be significantly modified by the presence of matter (at $O(\alpha)$).

The dominant effect will arise from the $(1-\alpha)^{-2}$ modification of the overall magnitude of the oscillation probability, since we assume that the available experimental information will not be able to properly “see” the position of the oscillation maximum. This implies that the ν_e appearance rate for a fixed value of $|U_{e3}|^2$ is enhanced [suppressed] with respect to the pure vacuum one if the neutrino mass hierarchy is normal ($\alpha > 0$) [inverted, ($\alpha < 0$)]. The opposite happens in the antineutrino channel. If the mass hierarchy is not known, a degeneracy in the determination of $|U_{e3}|^2$ surfaces, as a fixed value of $|U_{e3}|^2$ and a normal mass hierarchy will yield the same number of ν_e appearance events within some energy window as a larger value of $|U_{e3}|^2$ and an inverted mass hierarchy. This ambiguity can be solved by, for example, combining the information obtained with the neutrino and antineutrino channels (whose matter effects are opposite) or by changing the baseline of the experiment, such that the significance of the matter effect is modified. Note that precise information regarding the location (*i.e.*, the incoming neutrino energy) of the minimum of the ν_μ survival probability and the maximum of the ν_e appearance probability will also identify the neutrino mass hierarchy. This information, however, is hard to obtain in the appearance channel.

Another degeneracy ensues if $\sin^2 \theta_{23} \neq 0.5$. This comes from the fact that Eq. (III.8) is directly proportional to $\sin^2 \theta_{23}$, while, as discussed in Sec. II (see Fig. 1) the disappearance channel cannot distinguish $\sin^2 \theta_{23}$ from $1 - \sin^2 \theta_{23}$ (ignoring small $|U_{e3}|^2$ corrections). This means that for every $(|U_{e3}|^2, \sin^2 \theta_{23})$ pair there is another choice for the oscillation parameters (namely, $(|U_{e3}|^2 \tan^2 \theta_{23}, \cos^2 \theta_{23})$) which yields exactly the same $P(\nu_\mu \rightarrow \nu_e)$ as a function of energy, as long as the approximations that go into writing Eq. (III.8) apply. Contrary to the “hierarchy degeneracy,” the degeneracy in the atmospheric angle cannot be solved by comparing conjugated channels, as it is not modified by the presence of matter. Similar experiments at different baselines and neutrino energies will also have no effect. In order to eliminate this degeneracy it is necessary to either look at different oscillation modes (which come with distinct θ_{23} dependences) or to probe $P(\nu_\mu \rightarrow \nu_e)$ around $\alpha = 1$, where the value of $|U_{e3}|^2$ affects the ν_e appearance rate in a less trivial way.

Candidates for different oscillation modes include the search for the disappearance of electron-type neutrinos or $\nu_e \leftrightarrow \nu_\tau$ oscillations. For $|U_{e3}|^2 \ll 1$

$$P(\nu_e \rightarrow \nu_e) = 1 - \frac{4s_{13}^2}{(1-\alpha)^2} \sin^2 [\Delta_{23}(1-\alpha)], \quad (\text{III.9})$$

$$P(\nu_e \rightarrow \nu_\tau) = c_{23}^2 \frac{4s_{13}^2}{(1-\alpha)^2} \sin^2 [\Delta_{23}(1-\alpha)], \quad (\text{III.10})$$

which depend only on $|U_{e3}|^2$ or on $\cos^2 \theta_{23}|U_{e3}|^2$. We will comment more on this issue in the next section.

IV. SIMULATIONS OF THE OFF-AXIS EXPERIMENT(S)

We simulate and analyse “data” for electron (anti)neutrino appearance in a highly segmented iron-scintillator detector located off-axis from the NuMI neutrino beam. The detector is described in [16], together with the off-axis

neutrino beams and the reconstruction efficiencies, and we refer readers to it for more details. We will always assume that the data consists of 120 kton-years of running with a “neutrino beam” (see [16]) plus, whenever applicable, 300 kton-years of running with an “antineutrino beam.” We assume that the detector is located 12 km off-axis and 900 km away from the neutrino source (see [16]), unless otherwise noted. We further include in the “data” analysis the fact that $|\Delta m_{13}^2|$ is measured with a precision of $\Delta(|\Delta m_{13}^2|) = 0.1 \times 10^{-3} \text{ eV}^2$, while $\sin^2 2\theta_{23}^{\text{eff}}$ is measured with a precision $\Delta(\sin^2 2\theta_{23}^{\text{eff}}) = 0.01$. This type of precision has been quoted, for example, in studies of the physics capabilities of a future JHF to SuperKamiokande neutrino program [17], and we assume that the study of muon disappearance at the off-axis detector being considered here should yield similar precision. Both errors are considered to be one sigma, uncorrelated, Gaussian errors.[‡]

In order to discuss all relevant physics issues, we will consider several scenarios: $\sin^2 \theta_{23} = 0.35, 0.5, 0.65$, $\Delta m_{13}^2 = \pm(2, 3, 4) \times 10^{-3} \text{ eV}^2$ and $|U_{e3}|^2 < 0.05$. These choices are meant to be close to the current best fit of the atmospheric neutrino data [4, 7] or at the boundaries of the currently allowed 99% CL region. For concreteness, we have fixed $\Delta m_{12}^2 = 0.93 \times 10^{-7} \text{ eV}^2$, $\sin^2 \theta_{12} = 0.33$. It should be clear that any other LOW value for the solar parameters would have yielded identical results.

First, we determine the capability of the setup in question to observe a signal. We do that by computing the sensitivity to ν_e appearance as a function of the relevant oscillation parameters. The three sigma sensitivity CL curve for 120 kton-years of neutrino-beam running (see [16] for details) is depicted in Fig. 2 in the $(|U_{e3}|^2 \times \Delta m_{13}^2)$ -plane, for both neutrino mass hierarchies (signs of Δm_{13}^2) and three different values of $\sin^2 \theta_{23}$. By sensitivity we mean that, if $|U_{e3}|^2, \Delta m_{13}^2$ correspond a point in the curve, the probability that the number of events observed after 120 kton-years of running is due to background is 0.27%.

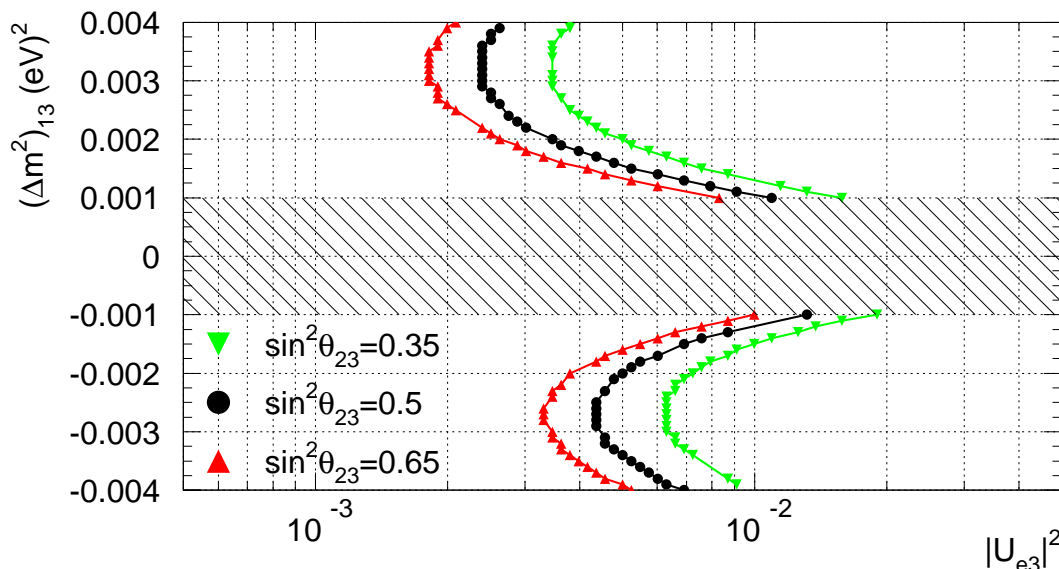


FIG. 2: Three sigma confidence level sensitivity of 120 kton-years of “neutrino beam” data, 12 km off-axis and 90 km away from the NuMI beam, as a function of Δm_{13}^2 and $|U_{e3}|^2$, for $\sin^2 \theta_{23} = 0.35, 0.5, 0.65$. The hatched region is currently ruled out by the atmospheric neutrino data at the three sigma confidence level.

As discussed in Sec. III, the sensitivity is greater for larger values of $\sin^2 \theta_{23}$ and for the normal neutrino mass hierarchy, due to a larger number of ν_e -appearance candidates. Not surprisingly, Fig. 2 indicates that the optimal sensitivity occurs for $\Delta m_{13}^2 \simeq 3 \times 10^{-3} \text{ eV}^2$, as we have chosen the neutrino-beam energy profile (*i.e.*, the off-axis distance) and experimental baseline in order to obtain $\Delta_{13} \simeq \pi/2$ for this particular value of the mass-squared difference.

Once a signal is detected, the next step is to try and determine the neutrino mixing parameters, Δm_{13}^2 , $|U_{e3}|^2$ and $\sin^2 \theta_{23}$. We do this for several different input values. The two-sigma confidence level measurements in the

[‡] As noted in Sec. II, a Gaussian error in $\sin^2 2\theta_{23}$ does not leads to a Gaussian error for $\sin^2 \theta_{23}$. This is appropriately taken into account.

$(\Delta m_{13}^2 \times |U_{e3}|^2)$, $(|U_{e3}|^2 \times \sin^2 \theta_{23})$, and $(\Delta m_{13}^2 \times \sin^2 \theta_{23})$ -planes obtained after 120 kton-years of “neutrino-beam data” are depicted in Figs. 3, 4, and 5, for $\sin^2 \theta = 0.5$, 0.35, and 0.65, respectively, $\Delta m_{13}^2 = +3 \times 10^{-3} \text{ eV}^2$ and $|U_{e3}|^2 = 0.008$. In the case of “maximal” atmospheric mixing (Fig. 3), there are still two disconnected solutions, centered around two distinct values of Δm_{13}^2 and $|U_{e3}|^2$. In this case, one would obtain at the two-sigma level $0.005 < |U_{e3}|^2 < 0.02$. For nonmaximal atmospheric mixing (Figs. 4, 5), the situation is even more confusing, and there are four disconnected solutions centered at distinct values of all the three parameters of interest.

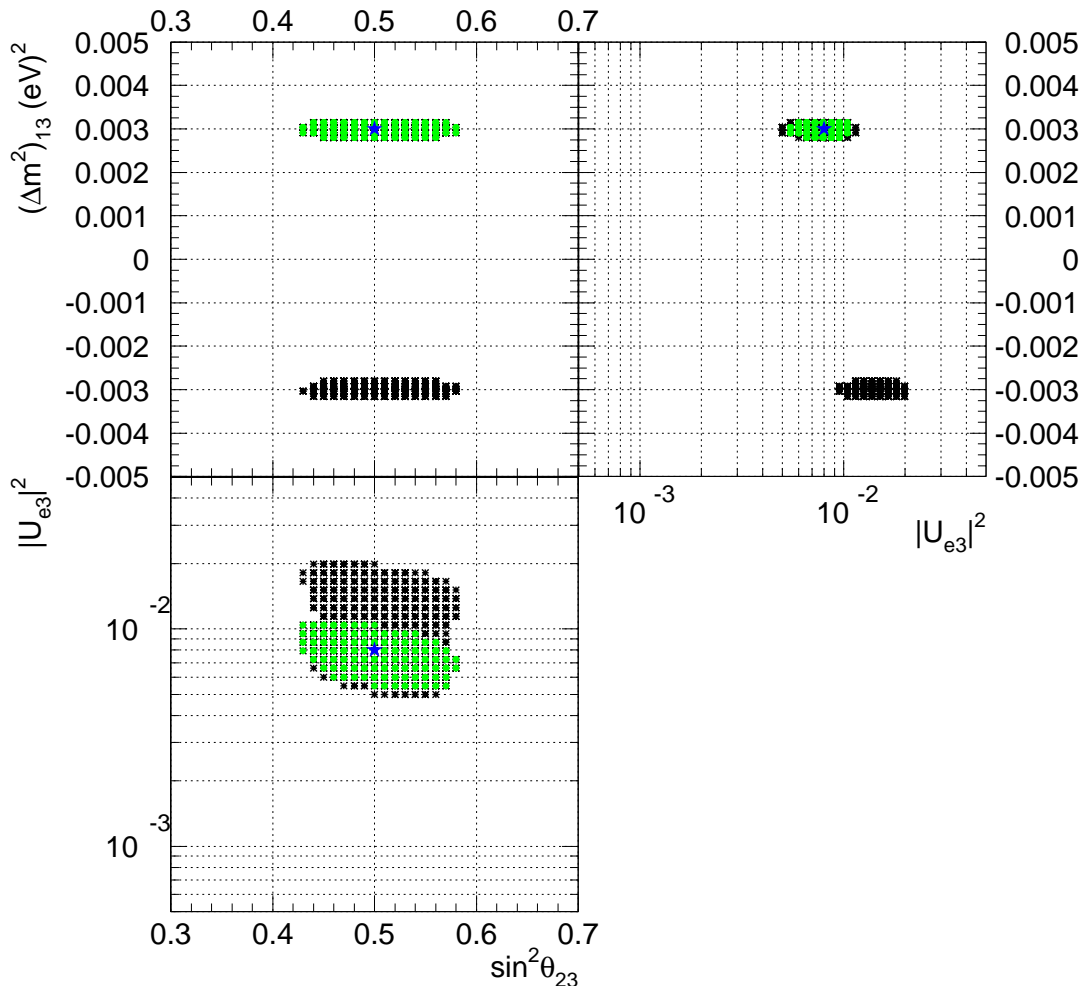


FIG. 3: Two-sigma confidence level regions in the $(\Delta m_{13}^2 \times |U_{e3}|^2)$, $(|U_{e3}|^2 \times \sin^2 \theta_{23})$, and $(\Delta m_{13}^2 \times \sin^2 \theta_{23})$ -planes obtained after 120 kton-years of “neutrino-beam data” (dark squares) combined with 300 kton-years of “antineutrino-beam data” (light [green] circles) for the following input value for the mixing parameters (indicated by the [blue] stars): $\Delta m_{13}^2 = 3 \times 10^{-3} \text{ eV}^2$, $|U_{e3}|^2 = 0.008$, and $\sin^2 \theta_{23} = 0.5$. See text for details.

Several other comments can be made regarding Figs. 3, 4, and 5. First, as hinted in Sec. II, the size of the $\sin^2 \theta_{23}$ uncertainty is significantly larger for maximal atmospheric mixing than for the nonmaximal cases. Second, even though $\sin^2 \theta_{23} = 0.35$ and $\sin^2 \theta_{23} = 0.65$ yield approximately the same value of $\sin^2 2\theta_{23}^{\text{eff}}$ and therefore similar number of disappearing ν_{μ} s (see Sec. II), they yield very different number of appearing ν_e s, as discussed in Sec. III. This fact is clearly visible if one compares Figs. 4, 5. The error contours are smaller for $\sin^2 \theta_{23} = 0.65$ (Fig. 5) given the larger statistics.

In order to “solve” the degeneracies, more information is needed. One option is to run with an antineutrino beam and keep the same experimental setup, or perform a different experiment with a different baseline and neutrino beam. We will here pursue the first option, but warn readers that running with antineutrinos takes a significantly larger amount of running time in order to obtain the same amount of data (especially if the neutrino mass hierarchy is

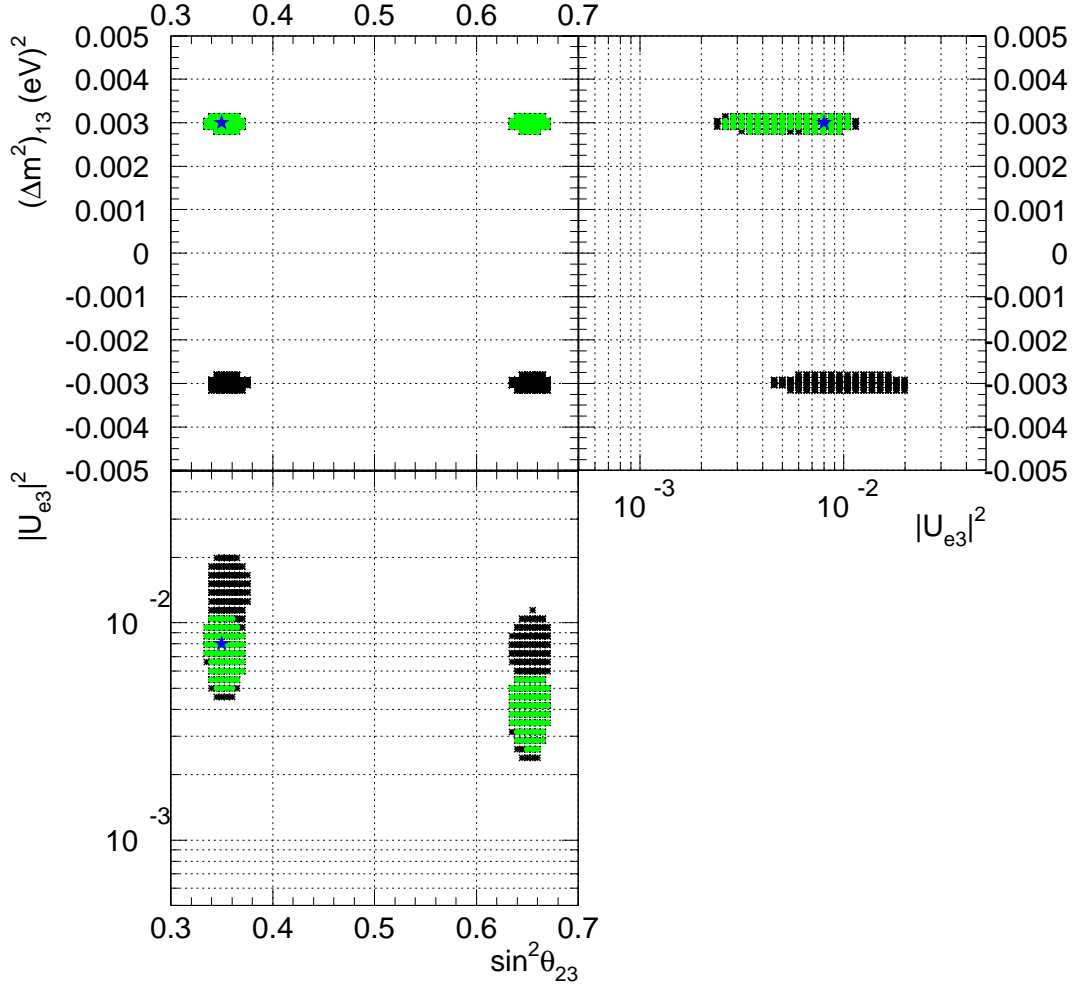


FIG. 4: Same as Fig. 3, for $\sin^2 \theta_{23} = 0.35$.

normal). In our opinion, antineutrino running is only realistic if an improved proton driver, such as the one currently being investigated [24] was present at NuMI. The existence of another experiment with a different neutrino beam and baseline might turn out to be realistic if the JHF to SuperKamiokande proposal materializes.

We depict the two-sigma CL measurements in the $(\Delta m^2_{13} \times |U_{e3}|^2)$, $(|U_{e3}|^2 \times \sin^2 \theta_{23})$, and $(\Delta m^2_{13} \times \sin^2 \theta_{23})$ -planes obtained after 120 kton-years of “neutrino-beam data” and 300 kton-years of “antineutrino-beam data” in Figs. 3, 4, and 5. One can see that in the case of maximal atmospheric mixing (Fig. 3) the two-fold degeneracy is lifted, and not only does one obtain a better measurement of $|U_{e3}|^2$ but, more importantly (in our opinion), one can determine the neutrino mass-hierarchy. In the case of non-maximal atmospheric mixing, the four-fold degeneracy collapses to a two-fold degeneracy, and the neutrino mass hierarchy can also be unambiguously measured.

The capability of determining the neutrino mass hierarchy will depend on the size of $|U_{e3}|^2$. Fig. 6 depicts the value of $\Delta\chi^2 \equiv |\chi^2_{\min}(\Delta m^2_{13} < 0) - \chi^2_{\min}(\Delta m^2_{13} > 0)|$ as a function of the input value of $|U_{e3}|^2$, assuming that the real value of $\Delta m^2_{13} = +3 \times 10^{-3} \text{ eV}^2$. $\Delta\chi^2$ is defined after integrating out the marginal parameters $|U_{e3}|^2$ and $\sin^2 \theta_{23}$, and is to be interpreted as a $\Delta\chi^2$ for one degree of freedom (Δm^2_{13}).[§] This means that, if $\sin^2 \theta_{23} = 0.5$, a two sigma hint that the neutrino mass hierarchy is normal should be obtained if $|U_{e3}|^2 = 0.003$, while a five sigma discovery

[§] This is distinct from the analysis presented in [16].

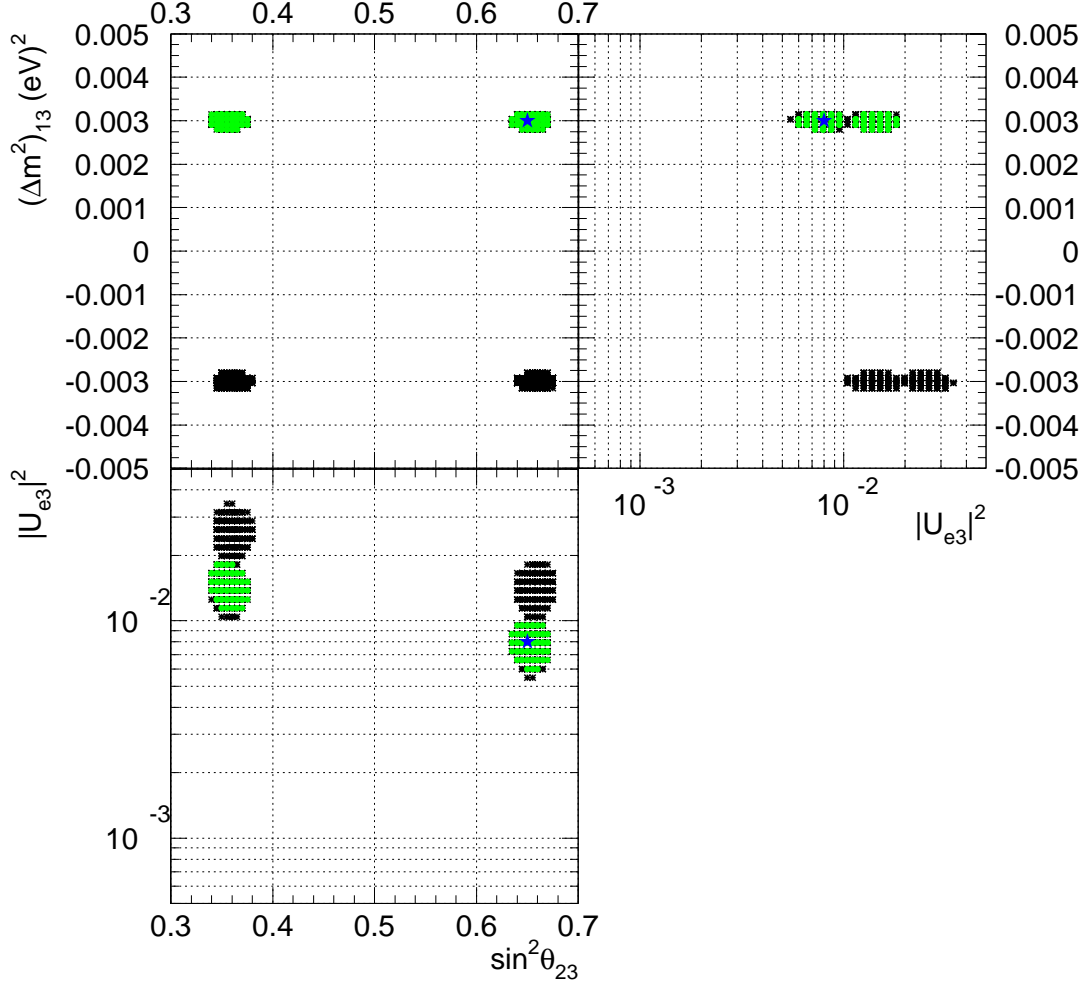


FIG. 5: Same as Fig. 3, for $\sin^2 \theta_{23} = 0.65$.

of the neutrino mass ordering should be achieved if $|U_{e3}|^2 \gtrsim 0.009$. The discriminatory power depends on the value of $\sin^2 \theta_{23}$, and increases with increasing $\sin^2 \theta_{23}$. As has been pointed out in Sec. III, this is due to the fact that the number of ν_e events due to oscillations is proportional to $\sin^2 \theta_{23}$, and more statistics can be obtained after the same running time for larger values of $\sin^2 \theta_{23}$. Note that this is true even though the solution with $\sin^2 \theta_{23} \neq 0.5$ (statistically) is still ambiguous when it comes to determining the value of $|U_{e3}|^2$ and whether $\theta_{23} > \pi/4$ or $\theta_{23} < \pi/4$.

As mentioned in Sec. III, solving the $\theta_{23} \leftrightarrow \pi/2 - \theta_{23}$ degeneracy is much trickier. It is not resolved by comparing the neutrino channel with the antineutrino channel, or even comparing different searches for $\nu_\mu \rightarrow \nu_e$ -transitions in long-baseline experiments, as long the matter effects are far from the $\alpha \sim 1$ “resonance” region. In order to probe such a regime, however, one is forced to probe very large neutrino energies, and hence very long neutrino baselines, which implies the construction of new, futuristic, neutrino facilities.

As we pointed out in Sec. III, other options include looking for $\nu_e \rightarrow \nu_\tau$ -transitions [25]. In order to accomplish this, it is necessary to build an intense, high energy source of electron-type neutrinos, *i.e.*, a neutrino factory. One would have to decide, however, if the construction of such a device is worthwhile given its physics capabilities in the scenario

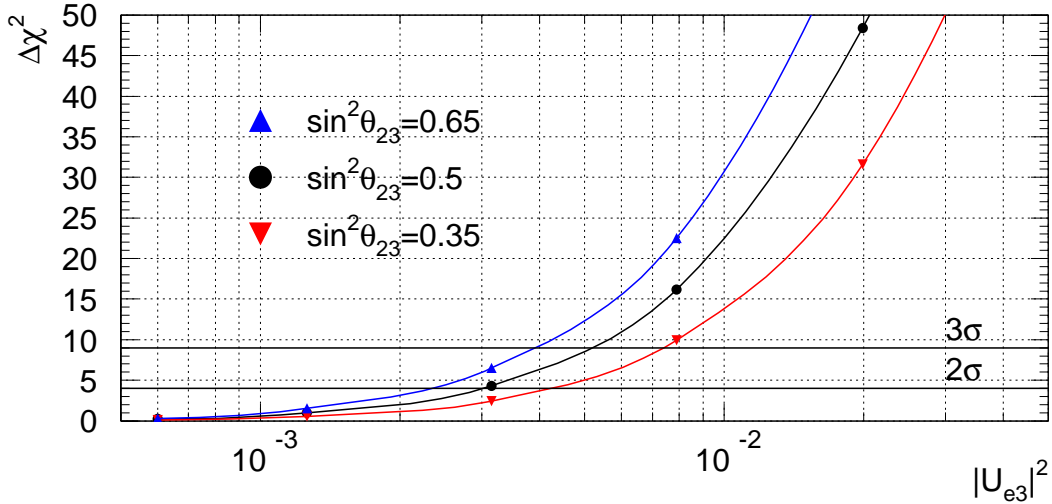


FIG. 6: $\Delta\chi^2 \equiv |\chi^2_{\min}(\Delta m_{13}^2 < 0) - \chi^2_{\min}(\Delta m_{13}^2 > 0)|$ as a function of $|U_{e3}|^2$, for $\Delta m_{13}^2 = +0.003 \text{ eV}^2$ and $\sin^2 \theta_{23} = 0.35, 0.5, 0.65$, obtained after 120 kton-years of “neutrino beam data” and 300 kton-years of “antineutrino beam data.” See text for details. The solid horizontal lines indicate the two- and three-sigma confidence levels for determining the sign of Δm_{13}^2 .

we are considering here.[¶]

One final option would be to study the disappearance of electron-type (anti)neutrinos from nuclear reactors. Unlike, say, the KamLAND experiment, such reactor would not have to be a very long baseline setup, and CHOOZ-like distances ($O(1 \text{ km})$) would be optimal. The challenge would be, however, to improve the “ $\sin^2 2\theta$ -sensitivity” of the CHOOZ experiment by, say, a factor of 10, from $O(0.1)$ to $O(0.01)$. Such an experiment would have to deal, for example, with the issues which help define the sensitivity of the CHOOZ experiment, such as the overall neutrino flux normalization, which is nominally known to a few percent [19]. One way to try and address this issue would be to also include a near detector, *a la* Bugey [26].

Next, we would like to address a more “practical” but important issue, related to how well should the atmospheric parameters be measured before a “safe” decision regarding the location of the off-axis detector can be made. Part of the information required in order to address this issue is already contained in Fig. 2. One sees that the sensitivity worsens significantly for $|\Delta m^2| \lesssim 2 \times 10^{-3} \text{ eV}^2$ because the oscillation maximum begins to “leave” the energy window we are looking into, and the statistics begins to deteriorate significantly. A different question we would like to address is whether one can still try to obtain information regarding the neutrino mass hierarchy. We do this by repeating the analysis depicted in Fig. 6 for fixed $\sin^2 \theta_{23} = 0.5$ but significantly different values of Δm_{13}^2 . Fig. 7 depicts the value of $\Delta\chi^2$ as a function of the input value of $|U_{e3}|^2$ for $\Delta m_{13}^2 = +(2, 3, 4) \times 10^{-3} \text{ eV}^2$, which are meant to cover the currently allowed 99% CL measurement of $|\Delta m_{13}^2|$. A more precise measurement should be expected after a few more years of K2K data [21], and will definitely be obtained after MINOS [22] and the CNGS[23] experiments “turn on.”

One should note that, even for $\Delta m_{13}^2 = 0.002 \text{ eV}^2$, where the statistics is expected to be significantly worse, a three sigma effect can be obtained for $|U_{e3}|^2 \gtrsim 0.01$. For $\Delta m_{13}^2 = 0.004 \text{ eV}^2$ it turns out that the discriminatory power is larger than for $\Delta m_{13}^2 = 0.003 \text{ eV}^2$, even though the statistical sample is slightly smaller. This is due to the fact that for $\Delta m_{13}^2 = 0.004 \text{ eV}^2$ the maximum of the oscillation takes place at a larger value of the neutrino energy (compared with the “optimal” $\Delta m_{13}^2 = 0.003 \text{ eV}^2$), such that when the mass hierarchy is inverted, the oscillation maximum starts to “leave” the energy window we are looking into. This means that the number of events obtained with the other choice neutrino mass-hierarchy is “more different” than in the case $\Delta m_{13}^2 = 0.003 \text{ eV}^2$, improving the discriminatory power. Incidentally, the same phenomenon renders the discriminatory power in the case $\Delta m_{13}^2 = 0.002 \text{ eV}^2$ worse. Note that this effect came about because we chose the input value of Δm_{13}^2 to be positive. Were Δm_{13}^2 negative, we would

[¶] We do not advocate that there is no case for building a neutrino factory if the LMA solution is ruled out. We do believe, however, that its physics goals would have to be reviewed in detail. This statement, of course, only applies if no other new physics is discovered in the leptonic sector until then.

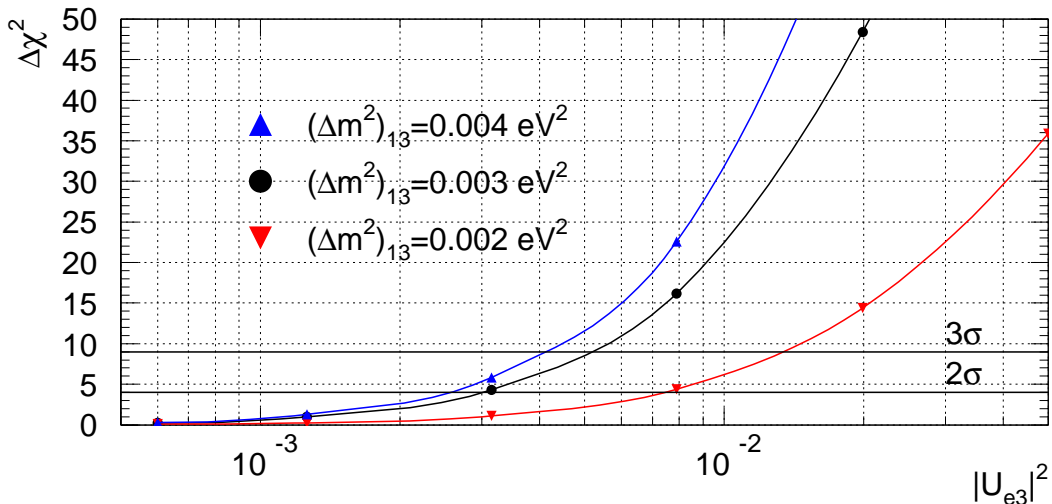


FIG. 7: Same as Fig. 6, for $\sin^2 \theta_{23} = 0.5$ and $\Delta m_{13}^2 = 0.002, 0.003, 0.004 \text{ eV}^2$.

have observed the opposite trend.

Finally, one may also inquire what happens if the baseline were different from the 900 km we have chosen here. It turns out that for distances which are slightly smaller than 900 km ($L \gtrsim 700 \text{ km}$) similar results can be obtained, as was discussed in detail in [16]. For significantly smaller baselines ($L \lesssim 500 \text{ km}$), however, the matter effects become less significant, and the “optimal” energy for a fixed value of Δm_{13}^2 becomes significantly smaller. This implies that while one might still keep the sensitivity to observing $|U_{e3}|^2$ to similar levels, the power to discriminate between the two neutrino mass-hierarchies disappears. Furthermore, it should be added that performance for the iron-scintillator detector we are assuming for neutrino energies between 1 and 3 GeV does not apply for an equivalent energy window centered below 1 GeV, as the capability to distinguish electrons from neutral current events (and even muons) deteriorates. In this sub-GeV regime, one might be better off using different detector technologies, such as Water Cherenkov detectors (as is being proposed for the JHK to SuperKamiokande project)**

V. CONCLUDING REMARKS

In the most conservative of scenarios, the fact that neutrinos have mass and mix will be confirmed as the solution to the atmospheric and solar neutrino puzzles, while the LSND result will be ruled out as a signal for neutrino oscillations. In such a world, the main goal of the next generation of neutrino oscillation experiments is very clear: measure (or further constrain) the “small” U_{e3} element of the leptonic mixing matrix. This is true irrespective of what the solution to the solar neutrino puzzle is. If the solar mass-squared difference is large enough, there is also the exciting “bonus” of trying to probe CP-violation in the leptonic sector.

If the solution to the solar neutrino puzzle requires a very small $\Delta m_{\text{solar}}^2$, CP violation becomes inaccessible, as “solar effects” simply cannot be observed in terrestrial experiments. Nonetheless, we have shown that the physics prospects for future long-baseline neutrino experiments are still very attractive. In many respects, measuring U_{e3} becomes a simpler task, while several obstacles still remain. While overcoming these obstacles, we have shown that one can (must) not only measure $|U_{e3}|^2$ in long-baseline experiments with non-negligible matter effects, but also determine the neutrino mass-hierarchy. Determining the mass hierarchy is arguably the second clear goal of future neutrino experiments (whether or not neutrino oscillations are directly involved) and just as exciting (in our opinion), as discovering CP-violation in the leptonic sector. Whether or not the neutrino mass-hierarchy is normal or inverted is certainly cleaner to address if “solar effects” are not around to complicate things, and requires information from two

** We thank Michal Szleper for comments concerning detector performance issues.

distinct oscillation channels, such as $\nu_\mu \rightarrow \nu_e$ -transitions at a long baseline, complemented by $\bar{\nu}_\mu \rightarrow \bar{\nu}_e$ -transitions at the same experiment. Another option is to combine a “long” and a “short” long-baseline search for $\nu_\mu \rightarrow \nu_e$ -transitions. This might well be the scenario that we will contemplate in the future if both the JHF to SuperKamiokande and the NuMI off-axis efforts materialize.

We have included the effects of “translating” the information obtained in the disappearance channel to the appearance channel, error bars included. Not only can we cleanly identify the confusion induced by not knowing what the neutrino mass-hierarchy is, but also identify the θ_{23} versus $\pi/2 - \theta_{23}$ degeneracy [18], which proves to be much harder to lift in the type of long-baseline experiments we (and most of the community) imagine as feasible in the near to intermediate future. We do provide a few candidate solutions, which involve new neutrino oscillation experiments, such as a “Super-Bugey” effort [26] or hunting for $\nu_e \rightarrow \nu_\tau$ transitions. Finally, it should be noted, of course, that several of the issues we raise here are also applicable if the LMA solution is confirmed by KamLAND.

In summary, the results of the KamLAND experiment (and, in a few years, of MiniBoone [27]) will shape the future of neutrino physics experiments. If we are on the right track (*i.e.*, if there are no major surprises or setbacks), however, all different roads seem to lead to a next-generation, long-baseline experiment capable of searching for $\nu_\mu \leftrightarrow \nu_e$ -oscillations. Even if the LMA solution is ruled out, several fundamental measurements can be performed by such experiments, which are worthy of very serious consideration.

Acknowledgments

This work was supported by the U.S. Department of Energy Grant DE-AC02-76CHO3000. It is a pleasure to thank Michal Szleper and Mayda Velasco for collaboration in early stages of this work as well as for “experimental” inputs throughout. We are also grateful to Bob Bernstein for comments regarding the extraction of the atmospheric parameters from the disappearance channel, to Maury Goodman for carefully reading the manuscript and providing many important comments, and to Hisakazu Minakata, for discussions regarding future reactor experiments and comments on the manuscript.

APPENDIX A: OSCILLATION PROBABILITIES AND THE LOW SOLUTION

The effective Hamiltonian that describes the time evolution of neutrinos in matter can be written in the flavor basis as

$$H = \frac{1}{2E} \left\{ U \begin{pmatrix} 0 & & \\ & \Delta m_{12}^2 & \\ & & \Delta m_{13}^2 \end{pmatrix} U^\dagger + \begin{pmatrix} a & & \\ & 0 & \\ & & 0 \end{pmatrix} \right\}, \quad (\text{A.1})$$

where $a = G_F \sqrt{2} N_e 2E$ represents matter effects from the effective potential of electron-neutrinos with electrons, and U is the flavor mixing matrix in vacuum (PDG representation),

$$U = \begin{pmatrix} c_{12}c_{13} & s_{12}c_{13} & s_{13}e^{-i\delta} \\ -s_{12}c_{23} - c_{12}s_{23}s_{13}e^{i\delta} & c_{12}c_{23} - s_{12}s_{23}s_{13}e^{i\delta} & s_{23}c_{13} \\ s_{12}s_{23} - c_{12}c_{23}s_{13}e^{i\delta} & -c_{12}s_{23} - s_{12}c_{23}s_{13}e^{i\delta} & c_{23}c_{13} \end{pmatrix}. \quad (\text{A.2})$$

By imposing $|\Delta m_{13}^2| > \Delta m_{12}^2 > 0$, we can relate θ_{23} and $|\Delta m_{13}^2|$ with the atmospheric angle and mass-squared difference, θ_{12} and Δm_{12}^2 with the solar angle and mass-square difference, and θ_{13} with the “reactor” angle. These definitions are used throughout the paper (see [16] for details).

For a baseline L , the evolution of neutrino states is given by

$$\nu(L) = S(L)\nu(0), \quad (\text{A.3})$$

with

$$S(L) = e^{-iHL} \quad (\text{A.4})$$

for constant matter density. The corresponding effective Hamiltonian for antineutrinos is obtained by $U \rightarrow U^*$ and $a \rightarrow -a$.

If the Hamiltonian can be separated into $H = H_0 + \epsilon H_1$, where H_0 can be exactly solved and $\epsilon \ll 1$ such that H_1 can be appropriately treated in perturbation theory, then $S(L) = S_0(L) + S_1(L)$ and $S_0(L) = e^{-iH_0 L}$ gives the lowest order transition amplitudes.

For $|\Delta m_{12}^2| \ll |dm_{13}^2|$, and non negligible a , we choose

$$\begin{aligned} H_0 &= \frac{1}{2E} \left\{ U \begin{pmatrix} 0 & & \\ & 0 & \\ & & \Delta m_{13}^2 \end{pmatrix} U^\dagger + \begin{pmatrix} a & & \\ & 0 & \\ & & 0 \end{pmatrix} \right\} \\ &= \frac{1}{2E} \tilde{U} \begin{pmatrix} 0 & & \\ & \Delta \tilde{m}_2^2 & \\ & & \Delta \tilde{m}_3^2 \end{pmatrix} \tilde{U}^\dagger, \end{aligned} \quad (\text{A.5})$$

where $\Delta \tilde{m}^2$ describes the energy-level spacing in matter and \tilde{U} the effective mixing elements, and ignore H_1 effects, which are suppressed by $\epsilon = \Delta m_{12}^2 / \Delta m_{13}^2$. Of course,

$$S_0(L) = \tilde{U} \begin{pmatrix} 0 & & \\ & e^{-i \frac{\Delta \tilde{m}_2^2}{2E} L} & \\ & & e^{-i \frac{\Delta \tilde{m}_3^2}{2E} L} \end{pmatrix} \tilde{U}^\dagger. \quad (\text{A.6})$$

The exact diagonalization of H_0 yields the effective mass differences and mixing angles in matter in the limit $|\Delta m_{12}^2 / \Delta m_{13}^2| \rightarrow 0$, while no approximation have to be made regarding a . One obtains

$$\tilde{U} = \begin{pmatrix} 0 & \frac{e^{-i\delta}}{n_2} (l_2 - c_{13}^2) & \frac{e^{-i\delta}}{n_3} (l_3 - c_{13}^2) \\ -c_{23} & \frac{1}{n_2} s_{23} s_{13} c_{13} & \frac{1}{n_3} s_{23} s_{13} c_{13} \\ s_{23} & \frac{1}{n_2} c_{23} s_{13} c_{13} & \frac{1}{n_3} c_{23} s_{13} c_{13} \end{pmatrix}, \quad (\text{A.7})$$

for the mixing angles in terms of the vacuum parameters, where we have defined

$$n_2 = \sqrt{l_2^2 - 2l_2 c_{13}^2 + c_{13}^2}; \quad n_3 = \sqrt{l_3^2 - 2l_3 c_{13}^2 + c_{13}^2}, \quad (\text{A.8})$$

and

$$\begin{aligned} l_2 &\equiv \frac{\Delta \tilde{m}_2^2}{\Delta m_{13}^2} = \frac{1}{2} \left[1 + \alpha - \sqrt{1 + \alpha^2 - 2\alpha \cos(2\theta_{13})} \right]; \\ l_3 &\equiv \frac{\Delta \tilde{m}_3^2}{\Delta m_{13}^2} = \frac{1}{2} \left[1 + \alpha + \sqrt{1 + \alpha^2 - 2\alpha \cos(2\theta_{13})} \right], \end{aligned} \quad (\text{A.9})$$

which give the effective mass differences. We have introduced the dimensionless parameter $\alpha \equiv \frac{a}{\Delta m_{13}^2}$ for the sake of simplicity. The ordering of levels in matter is (1,2,3) for the hierarchical case of $\Delta m_{13}^2 > 0$ and $\alpha < 1$.

The effective mixing matrix \tilde{U} is independent of θ_{12} and δ , if the latter is appropriately rotated away. The matrix \tilde{U} can be expressed also in the PDG form. To do so, we change

$$\tilde{U} \rightarrow \tilde{U} \begin{pmatrix} 1 & & \\ & e^{i\delta} & \\ & & 1 \end{pmatrix}. \quad (\text{A.10})$$

By comparing with previous expressions, we may establish the correspondence between the effective mixing angles, $\tilde{\theta}_{ij}$, and the vacuum parameters, getting

$$\begin{aligned} \tilde{c}_{12} &= 0, & |\tilde{s}_{12}| &= 1, \\ \tilde{c}_{23} &= c_{23}, & \tilde{s}_{23} &= s_{23}, \\ \tilde{c}_{13} &= \frac{l_2 - c_{13}^2}{n_2}, & \tilde{s}_{13} &= \frac{l_3 - c_{13}^2}{n_3}, \end{aligned} \quad (\text{A.11})$$

up to signs. The vanishing mixing in matter $\tilde{c}_{12} = 0$ is a consequence of the degeneracy $\Delta m_{12}^2 = 0$ in vacuum and says that the lowest mass eigenstate in matter contains no electron-neutrino flavor component. This result is the ingredient that avoids genuine CP violation in matter, even if one has three non-degenerate effective masses.

The transition amplitudes for $\nu_\alpha \rightarrow \nu_\beta$ in the $\Delta m_{12}^2 / \Delta m_{13}^2 \rightarrow 0$ case are given by S_0 matrix elements, which can be written

$$\begin{aligned} A(\alpha \rightarrow \beta; L) &= S_0(L)_{\beta\alpha} \\ &= \delta_{\beta\alpha} + \tilde{U}_{\beta 2} \tilde{U}_{2\alpha}^\dagger \left(e^{-i \frac{\Delta \tilde{m}_2^2}{2E} L} - 1 \right) + \tilde{U}_{\beta 3} \tilde{U}_{3\alpha}^\dagger \left(e^{-i \frac{\Delta \tilde{m}_3^2}{2E} L} - 1 \right). \end{aligned} \quad (\text{A.12})$$

From this expression we may calculate all probabilities,

$$P(\nu_e \rightarrow \nu_e) = 1 - \sin^2(2\tilde{\theta}_{13}) \sin^2[\tilde{\Delta}_{13}] \quad (\text{A.13})$$

$$P(\nu_\mu \rightarrow \nu_e) = s_{23}^2 \sin^2(2\tilde{\theta}_{13}) \sin^2[\tilde{\Delta}_{13}] \quad (\text{A.14})$$

$$P(\nu_\tau \rightarrow \nu_e) = c_{23}^2 \sin^2(2\tilde{\theta}_{13}) \sin^2[\tilde{\Delta}_{13}] \quad (\text{A.15})$$

$$P(\nu_\mu \rightarrow \nu_\mu) = 1 - s_{23}^4 \sin^2(2\tilde{\theta}_{13}) \sin^2[\tilde{\Delta}_{13}] - 2s_{23}^2 c_{23}^2 \left\{ 1 - \cos[\Delta_{13}(1+\alpha)] \cos[\tilde{\Delta}_{13}] \right. \\ \left. + \cos(2\tilde{\theta}_{13}) \sin[\Delta_{13}(1+\alpha)] \sin[\tilde{\Delta}_{13}] \right\} \quad (\text{A.16})$$

$$P(\nu_\tau \rightarrow \nu_\mu) = s_{23}^2 c_{23}^2 \left\{ 2 - 2 \cos[\Delta_{13}(1+\alpha)] \cos[\tilde{\Delta}_{13}] - \sin^2(2\tilde{\theta}_{13}) \sin^2[\tilde{\Delta}_{13}] \right. \\ \left. + 2 \cos(2\tilde{\theta}_{13}) \sin[\Delta_{13}(1+\alpha)] \sin[\tilde{\Delta}_{13}] \right\} \quad (\text{A.17})$$

$$P(\nu_\tau \rightarrow \nu_\tau) = 1 - c_{23}^4 \sin^2(2\tilde{\theta}_{13}) \sin^2[\tilde{\Delta}_{13}] - 2s_{23}^2 c_{23}^2 \left\{ 1 - \cos[\Delta_{13}(1+\alpha)] \cos[\tilde{\Delta}_{13}] \right. \\ \left. + \cos(2\tilde{\theta}_{13}) \sin[\Delta_{13}(1+\alpha)] \sin[\tilde{\Delta}_{13}] \right\} \quad (\text{A.18})$$

where

$$\tilde{\Delta}_{13} \equiv \Delta_{13} \sqrt{1 + \alpha^2 - 2\alpha \cos(2\theta_{13})}, \quad \text{with} \quad \Delta_{13} \equiv \frac{\Delta m_{13}^2 L}{4E}. \quad (\text{A.19})$$

and

$$\sin^2(2\tilde{\theta}_{13}) = 4 \frac{s_{13}^2 c_{13}^2}{1 + \alpha^2 - 2\alpha \cos(2\theta_{13})}. \quad (\text{A.20})$$

In order to get the corresponding expressions for antineutrinos, one simply exchanges $a \rightarrow -a$, *i.e.*, $\alpha \rightarrow -\alpha$. The effect of such a change in the probabilities comes from the different relative sign between mass and matter terms in H_0 . It is important to note that, *because we are disregarding Δm_{12}^2 effects* (which is perfectly justified, as we are interested in the LOW solution) the expressions for neutrinos and antineutrinos are exchanged when the neutrino mass hierarchy is “flipped”, *i.e.*,

$$P(\nu_\alpha \rightarrow \nu_\beta)[\Delta m_{13}^2] = P(\bar{\nu}_\alpha \rightarrow \bar{\nu}_\beta)[-\Delta m_{13}^2]. \quad (\text{A.21})$$

This behavior is a consequence of the fact that we are, in practice, dealing with an effective two-level system.

-
- [1] Homestake Coll. (B.T. Cleveland *et al.*), *Astrophys. J.* **496**, 505 (1998); GALLEX Coll. (W. Hampel *et al.*), *Phys. Lett. B* **447**, 127 (1999); V.N. Gavrin, for the SAGE Coll., *Nucl. Phys. B* (Proc. Suppl.) **91**, 36 (2001); E. Bellotti, for the GNO Coll., *Nucl. Phys. B* (Proc. Suppl.) **91**, 44 (2001); SuperKamiokande Coll. (S. Fukuda, *et al.*) *Phys. Rev. Lett.* **86**, 5651 (2001); **86** 5656 (2001); SNO Coll. (Q.R. Ahmad *et al.*), *Phys. Rev. Lett.* **87**, 071301 (2001); **89**, 011301 (2002).
 - [2] SNO Coll. (Q.R. Ahmad *et al.*), *Phys. Rev. Lett.* **89**, 011302 (2002).
 - [3] NUSEX Coll. (M. Aglietta *et al.*), *Europhys. Lett.*, **8**, 611 (1989); R. Becker-Szendy *et al.*, *Phys. Rev. D* **46**, 3720 (1992); Kamiokande Coll. (Y. Hirata *et al.*), *Phys. Lett. B* **280**, 146 (1992); Kamiokande Coll. (Y. Fukuda *et al.*), *Phys. Lett. B* **335**, 237 (1994); Frejus Coll. (K. Daum *et al.*), *Z. Phys. C* **66**, 417 (1995); W.A. Mann, for the Soudan 2 Coll., *Nucl. Phys. B* (Proc. Suppl.) **91**, 134 (2001); B.C. Barish, for the MACRO Coll., *Nucl. Phys. B* (Proc. Suppl.) **91**, 141 (2001).
 - [4] SuperKamiokande Coll. (Y. Fukuda *et al.*), *Phys. Lett. B* **433**, 9 (1998); *Phys. Rev. Lett.* **81**, 1562 (1998); **82**, 2644 (1999); *Phys. Lett. B* **467**, 185 (1999).
 - [5] LSND Coll. (C. Athanassopoulos *et al.*), *Phys. Rev. Lett.* **75**, 2650 (1995); **77**, 3082 (1996); **81**, 1774 (1998); W.C. Louis for the LSND Coll., *Nucl. Phys. B* (Proc. Suppl.) **91**, 198 (2001); LSND Coll. (A. Aguilar *et al.*), *hep-ex/0104049*.
 - [6] V. Barger *et al.*, *Phys. Lett. B* **537**, 179 (2002); P. Creminelli, G. Signorelli, and A. Strumia, *hep-ph/0102234* – updated version (April 2002); A. Bandyopadhyay *et al.*, *hep-ph/0204286*; J.N. Bahcall, M.C. Gonzalez-Garcia, and C. Peña-Garay, *hep-ph/0204314*; P. Aliani *et al.*, *hep-ph/0205053*; P.C. de Holanda and A.Yu. Smirnov, *hep-ph/0205241*; G.L. Fogli *et al.*, *hep-ph/0206162*; M.B. Smy, *hep-ex/0108053*.
 - [7] M. Maltoni, *et al.*, *hep-ph/0207227*.
 - [8] A. Strumia *et al.*, *Phys. Lett. B* **541**, 327 (2002). See also G.F. Fogli *et al.* in [6].

- [9] A. Piepke for the KamLAND Collaboration, Nucl. Phys. Proc. Suppl. **91**, 99-104 (2001); S. A. Dazeley for the KamLAND Coll., arXiv:hep-ex/0205041.
- [10] V. D. Barger, D. Marfatia and B. P. Wood, Phys. Lett. **B498**, 53 (2001); R. Barbieri and A. Strumia, JHEP **0012**, 016 (2000). H. Murayama and A. Pierce, Phys. Rev. **D 65**, 013012 (2002).
- [11] A. de Gouvêa and C. Peña-Garay, Phys. Rev. **D 64**, 113011 (2001); P. Aliani *et al.*, hep-ph/0207348.
- [12] H. Murayama and T. Yanagida, Phys. Lett. **B520**, 263 (2001); G. Barenboim *et al.*, hep-ph/0108199; G. Barenboim, L. Borisso and J. Lykken, hep-ph/0201080; A. Strumia, Phys. Lett. **B539**, 91 (2002).
- [13] G. Ranucci for the Borexino Coll., Nucl. Phys. **B** (Proc. Suppl.) **91**, 58 (2001).
- [14] A. de Gouvêa, A. Friedland and H. Murayama, Phys. Rev. **D 60**, 093011 (1999); JHEP **0103**, 009 (2001).
- [15] V. Barger, *et al.*, Phys. Rev. **D 22**, 2718 (1980); A. De Rujula, M.B. Gavela, and P. Hernandez, Nucl. Phys. **B547**, 21 (1999); P. Lipari, Phys. Rev. **D 61**, 113004 (2000); S. Dutta, R. Gandhi, and B. Mukhopadhyaya, Eur. Phys. J. **C18**, 405 (2000); D. Dooling *et al.*, Phys. Rev. **D 61**, 073011 (2000); M. Freund *et al.*, Nucl. Phys. **B578**, 27 (2000); I. Mocioiu and R. Shrock, Phys. Rev. **D62**, 053017 (2000); V. Barger *et al.*, Phys. Lett. **B485**, 379 (2000); Phys. Rev. **D 62**, 073002 (2000); **D63**, 033002 (2001); A. Cervera *et al.*, Nucl. Phys. **B579**, 17 (2000), Erratum-ibid. **B593**, 731 (2001); Z.-Z. Xing, Phys. Lett. **487**, 327 (2000); Phys. Rev. **D63**, 073012 (2000); A. Bueno, M. Campanelli, A. Rubbia, Nucl. Phys. **B589**, 577 (2000); P. Fishbane, Phys. Rev. **D 62**, 093009 (2000); P. Fishbane and P. Kaus, Phys. Lett. **B506**, 275 (2001); P. Fishbane and S. Gasiorowicz, hep-ph/0012230; M. Freund, P. Huber, M. Lindner, Nucl. Phys. **B615**, 321 (2001); J. Arafune, J. Sato, Phys. Rev. **D 55**, 1653 (1997); H. Minakata, H. Nunokawa, Phys. Rev. **D 57**, 4403 (1998); A. Romanino, Nucl. Phys. **B574** 675 (2000); S.M. Bilenky, C. Giunti, W. Grimus, Phys. Rev. **D 58**, 033001 (1998); K. Dick *et al.*, Nucl. Phys. **B562**, 29 (1999); M. Tanimoto, Phys. Lett. **B462**, 115 (1999); A. Donini *et al.*, Nucl. Phys. **B574**, 23 (2000); M. Koike, J. Sato, Phys. Rev. **D 61**, 073012 (2000), Erratum-ibid. **D62**, 079903 (2000); S.J. Parke, T.J. Weiler, Phys. Lett. **B501**, 106 (2001); T. Miura *et al.*, Phys. Rev. **D 64**, 013002 (2001); M. Koike, T. Ota, J. Sato, Phys. Rev. **D 65**, 053015 (2002); P. Lipari, Phys. Rev. **D 64**, 033002 (2001); J. Burguet-Castell *et al.*, hep-ph/0207080; K. Whisnant, J.M. Yang, and B.-L. Yong, hep-ph/0208193; M. Aoki, K. Hagiwara, and N. Okamura, hep-ph/0208223, and many more references therein.
- [16] G. Barenboim *et al.*, hep-ph/0204208.
- [17] See <http://neutrino.kek.jp/jhfnu>, in particular, Y. Itoh *et al.*, “Letter of Intent: A Long Baseline Neutrino Oscillation Experiment using the JHF 50 GeV Proton Synchrotron and the Super-Kamiokande Detector” (Feb. 2000); Y. Itoh *et al.*, “The JHF-Kamioka Neutrino Project”, hep-ex/0106019.
- [18] V. Barger *et al.*, Phys. Rev. **D 63**, 113011 (2001); V. Barger, D. Marfatia, and K. Whisnant, hep-ph/0206038; H. Minakata, H. Nunokawa, and S. Parke, hep-ph/0208163.
- [19] M. Apollonio *et al.*, Phys. Lett. **B420**, 397 (1998); Phys. Lett. **B466**, 415 (1999).
- [20] See for example, several talks at the “NuFact’02 Workshop Neutrino Factories based on Muon Storage Rings,” July 1–6, 2002, Imperial College, London, <http://www.hep.ph.ic.ac.uk/NuFact02/>, and “New Initiatives for the NuMI beam at Fermilab,” May 2–4, 2002, Fermilab, http://www-nu.mi.fnal.gov/fnal_minos/new_initiatives/new_initiatives.html.
- [21] S. H. Ahn *et al.*, Phys. Lett. **B511**, 178 (2001); K. Nishikawa, talk at the “XXth International Conference on Neutrino Physics and Astrophysics,” May 24–30, 2002, Munich, Germany, <http://neutrino2002.ph.tum.de/>. See also G. L. Fogli, E. Lisi and A. Marrone, Phys. Rev. **D 65**, 073028 (2002).
- [22] See <http://www-nu.mi.fnal.gov/>.
- [23] See <http://proj-cnsgs.web.cern.ch/proj-cnsgs/>.
- [24] G. Barenboim *et al.*, hep-ex/0206025.
- [25] A. Donini, D. Meloni, and P. Migliozzi, hep-ph/0206034.
- [26] K. Inoue, H. Minakata, F. Suekane, H. Sugiyama, and O. Yasuda, to appear.
- [27] See <http://www-boone.fnal.gov/>.